Electronic Supporting Information

Induced chirality at the surface: fixation of a dynamic *M*/*P* invertible helical Co_3 complex on SiO_2

Satoshi Muratsugu,[a,b] Kana Sawaguchi,[a,c] Takafumi Shiraogawa,[d] Shunsuke Chiba,[e] Yoko Sakata,[e,f] Sora Shirai,[a] Hiroshi Baba,[a] Masahiro Ehara,*[d] Shigehisa Akine,*[e,f] and Mizuki Tada*[a,b,c]

[a] Department of Chemistry, Graduate School of Science, Nagoya University, Furo-cho, Chikusa-ku, Nagoya, 464-8602 Aichi, Japan.
[b] Integrated Research Consortium on Chemical Science (IRCCS), Nagoya University, Furo-cho, Chikusa-ku, Nagoya, 464-8602 Aichi, Japan.
[c] Research Center for Materials Science (RCMS), Nagoya University, Furo-cho, Chikusa-ku, Nagoya, 464-8602 Aichi, Japan.
[d] Institute for Molecular Science/School of Physical Sciences, Graduate University for Advanced Studies, Myodaiji, Okazaki, 444-8585 Aichi, Japan.
[e] Graduate School of Natural Science & Technology, Kanazawa University, Kakuma, Kanazawa, 920-1192 Ishikawa, Japan.
[f] Nano Life Science Institute (WPI-NanoLSI), Kanazawa University, Kakuma-machi, Kanazawa 920-1192 Ishikawa, Japan.
E-mail: tada.mizuki.u6@f.mail.nagoya-u.ac.jp, akine@se.kanazawa-u.ac.jp, ehara@ims.ac.jp

1. Experimental Section

Materials and instruments

Chemicals were purchased from commercial sources (Wako Chemicals, TCI, and Kishida Reagents Chemicals) and used without further purification unless otherwise noted. All experimental works were performed in a glovebox or in standard Schlenk flasks under N_2 atmosphere. $[LCo_3(NHMe_2)_6](OTf)_3$ was prepared according to the literatures, and a *tris*-(saloph)-type organic cage ligand was represented as L.[1-4]

Preparation of ethylenediamine-functionalized SiO_2 (en-SiO_2)

A typical procedure is shown here. SiO_2 (2.0 g; Aerosil 200, Nippon Aerosil, Co. Ltd.) was calcined at 473 K for 2 h and cooled under vacuum. Absolute toluene (50 mL) and $H_2N(CH_2)_2NH(CH_2)_3Si(OCH_3)_3$ (0.6 g, 2.7 mmol) was added to the calcined SiO_2, and the mixture was stirred and refluxed for 24 h. After cooling to room temperature, the resulting sample was collected in a thimble filter tube inside a Schlenk flask, and the sample was washed with toluene in a Soxhlet extractor overnight and then washed with *n*-hexane in a similar way under N_2. The sample was dried at 298 K under vacuum. The obtained sample is denoted as **en-SiO_2**. The surface density of immobilized en was estimated to be 2.3-2.4 nm^{-2} by the elemental analysis of N.

Attachment of $[LCo_3(NHMe_2)_6](OTf)_3$ to en-SiO_2 (LCo_3/en-SiO_2)

A typical procedure is shown here. An absolute acetonitrile solution of $[LCo_3(NHMe_2)_6](OTf)_3$ (55 mg, 2.3×10^{-2} mmol) (2.3 mmol L^{-1}) was added to **en-SiO_2** (0.5 g) at 298 K. After stirring for 24 h at 298 K, the solvent was filtrated under N_2 and the solid sample was washed with 10 mL of acetonitrile and dried under vacuum. The obtained sample is denoted as **LCo_3/en-SiO_2**. The Co loadings of the prepared **LCo_3/en-SiO_2** were estimated to be 0.56-0.72 wt% by XRF.

Addition of chiral (*R*)- or (*S*)-1-phenylethylamine ((*R*) or (*S*)-A1) to LCo_3/en-SiO_2 (LCo_3((*R*) or (*S*)-A1)/en-SiO_2)

An absolute methanol solution of a chiral (*R*) or (*S*)-1-phenylethylamine ((*R*) or (*S*)-**A1**) (2.2×10^1 mmol L^{-1}, (*R*) or (*S*)-**A1**: 10 equiv. to $[LCo_3]$ unit on **LCo_3/en-SiO_2**) was added to **LCo_3/en-SiO_2** at 298 K. After stirring for 1 h at 298 K, the solvent was filtrated and the solid sample was dried under vacuum. The obtained sample is denoted as **LCo_3((*R*)** or **(*S*)-A1)/en-SiO_2**. The Co loading of **LCo_3((*R*)-A1)/en-SiO_2** was estimated to be 0.64 wt% from XRF when **LCo_3/en-SiO_2** with the Co loading of 0.72 wt% was used.

Impregnation of $[LCo_3(NHMe_2)_6](OTf)_3$ to SiO_2 (LCo_3/SiO_2)

The attachment of $[LCo_3(NHMe_2)_6](OTf)_3$ on non-functionalized SiO_2 was conducted in a similar way by using calcined SiO_2 without ethylenediamine moiety (calcined at 473 K for 2 h). During washing process, leaching of Co was found and the loading of remained Co species after the wash of the solid sample was less than 0.4 wt% estimated by XRF. The obtained sample is denoted as **LCo_3/SiO_2**.

Addition of chiral (*S*)- or (*R*)-3-amino-1,2-propanediol ((*R*) or (*S*)-A2) to LCo_3((*R*) or (*S*)-A2)/en-SiO_2

An absolute methanol solution of a chiral (*S*) or (*R*)-3-amino-1,2-propanediol ((*S*) or (*R*)-**A2**) (2.2×10^2 mmol L^{-1}, 100 equiv. to $[LCo_3]$ unit on **LCo_3((*R*)** or **(*S*)-A1/en-SiO_2**) was added to **LCo_3((*R*)** or **(*S*)-A1/en-SiO_2** at 298 K, respectively. After stirring for 2 h at 298 K, the solvent was removed in vacuo and the solid sample was dried under vacuum.

Characterization of SiO_2-supported LCo_3 complexes

Elemental analysis was carried out on MT-6 CHN CORDOR, Yanako Analytical Instruments Co. Co loading was estimated by XRF using a JEOL JSX-1000S spectrometer. Transmission UV-vis spectra of liquid samples and diffuse-reflectance (DR) UV-vis spectra of solid samples were measured on a JASCO V-550 spectrometer. Solid samples were enclosed in quartz cells under Ar atmosphere and DR UV-vis spectra were recorded by using an integrating sphere. DR CD spectra were measured on a JASCO J-820 spectrometer equipped with an integrating sphere unit. Solid samples were enclosed in quartz cells under Ar atmosphere and DR CD spectra were obtained after the subtraction of a DR CD spectrum of pure SiO_2 as background.

Co *K*-edge X-ray absorption near-edge structure (XANES) spectra were measured in a transmission mode at 298 K at the BL12C station of the Photon Factory at KEK-IMSS, Japan (2.5 GeV, 450 mA). X-rays from the storage ring were monochromatized using Si(111) double crystals. Ionization chambers with pure N_2 and N_2/Ar (50/50) were used to detect incident and transmitted X-rays, respectively. [$LCo_3(NHMe_2)_6$] was diluted with BN and SiO_2-supported samples were measured as neat. The XANES spectra were analysed using ATHENA.[5] The threshold energy was tentatively set at the inflection point of the Co *K*-edge (7709.5 eV),[6] and background subtraction was performed using the Autobk method and the spline smoothing algorithm in ATHENA.[7]

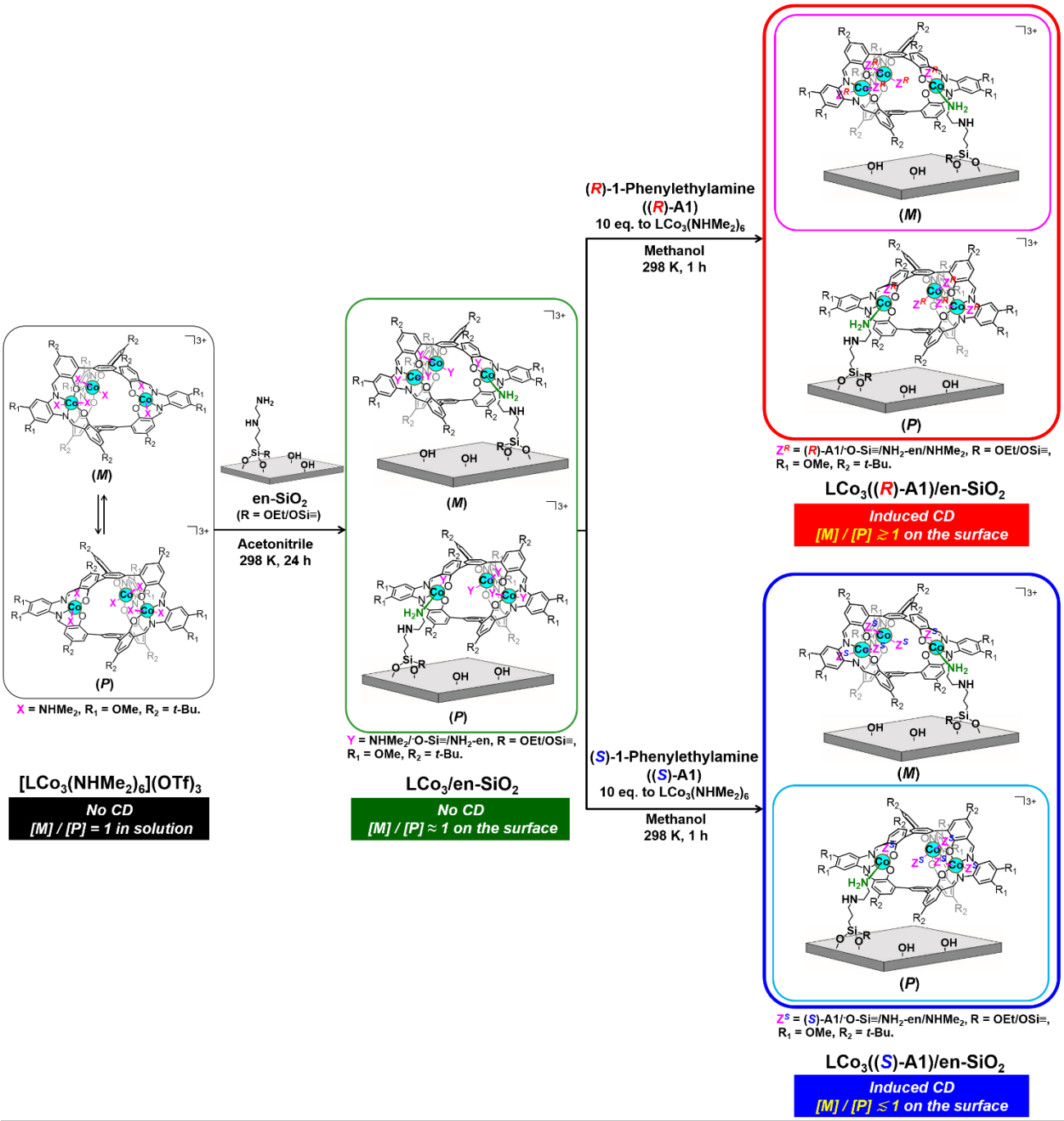

Scheme S1. Preparation of a supported helical LCo_3 complex, **LCo_3((*R*) or (*S*)-A1)/en-SiO_2**, by grafting of $[LCo_3(NHMe_2)_6](OTf)_3$ on an ethylenediamine-functionalized SiO_2 surface (**en-SiO_2**), followed by the addition of chiral (*R*) or (*S*)-1-phenylethylamine, respectively. Possible paired surface structures are presented.

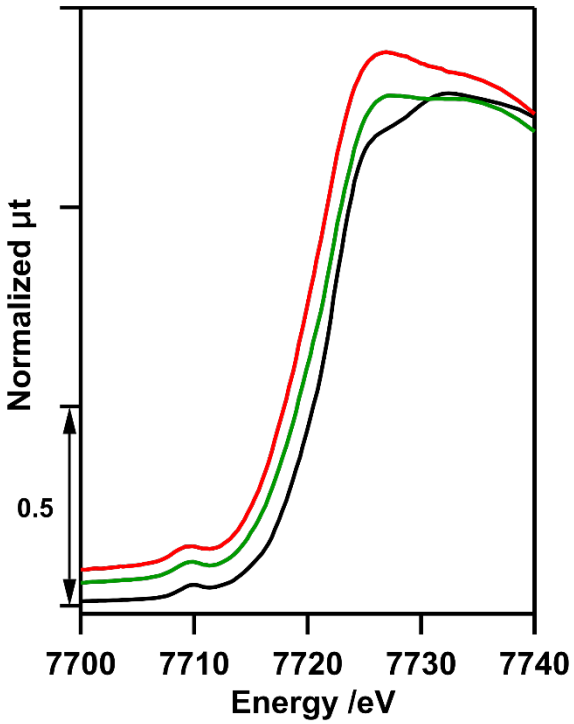

Fig. S1. Co *K*-edge XANES spectra of $[LCo_3(NHMe_2)_6](OTf)_3$ with BN (black), **LCo_3/en-SiO_2** (green), and **LCo_3((*R*)-A1)/en-SiO_2** (red).

2. Computational details

All the ground- and excited-state calculations were conducted using density functional theory (DFT) and time-dependent DFT (TD-DFT), respectively, with the B3LYP functional,[8] which is suitable for the valence excited states. The SDD[9] basis set with relativistic effective core potential (RECP) was employed for Co atom and 6-31G(d) basis set for the other atoms. Solvent effects were taken into account by the linear-response integral equation formalism-polarizable continuum model (LR-IEF-PCM) approach with non-equilibrium solvation.[10] Calculated electronic spectra for each transition were convoluted by overlapping Gaussians with half a band width at 1/*e* peak height of 0.1 eV for photo-absorption and 0.3 eV for circular dichroism (CD).[11] In the calculation of the CD spectrum, velocity-form rotatory strength was adopted to circumvent a problem of the gauge-origin dependence. For the absorption spectrum, length-form oscillator strength was employed because of its good basis set convergence. Ligand exchange-mediated stabilization was examined by Gibbs free energy at the standard condition.

To reduce calculation costs, $[LCo_3(NHMe_2)_6](OTf)_3$ was simplified by substituting *t*-butyl group of the L (saloph) ligand with methyl group and R_1 (OCH_3) group with hydroxyl group. A linker (3-(2-aminoethylamoni)propyltrimethoxysilane) for anchoring the LCo_3 complex on a SiO_2 surface was modelled by ethylenediamine ($H_2N(CH_2)_2NH_2$, abbreviated as en) in the simulation. The silanol group from the SiO_2 surface was modelled by $–O-Si(OH)_3$ in the simulation.

All the calculations were performed by using the Gaussian 16 Rev. A.03[12] suite of programs. Molecular structures were visualized by using the VMD software.[13]

The computations were partially performed in the Research Center for Computational Science, Okazaki, Japan (Project: 22-IMS-C185).

In the following section, the optimizes structures of trinuclear Co_3 complexes in solution and on the surface are abbreviated as follows, also as shown in **Fig. S2**;

The trinuclear Co_3 complex with ligand L: Dotted triangle with three Co centers

The torsion angle ω of saloph moiety: A dihedral angle of carbon atoms (a–b–c–d) of saloph moiety in L
ω has a negative value when helicity is *M*, ω has a positive value when helicity is *P*.

The axial ligands of Co, X: $NHMe_2$, **A1**, linker ligand ≡ ($NH_2(CH_2)_2NH_2$, coordination from SiO_2 surface ≡ –O-Si

The CD simulation with abundance ratio was performed by adding the *M* and *P*-configurated CD spectra using the following equation:

$$I_{sum} = c_M I_M + c_P I_P \quad \cdot\cdot\cdot \text{Equation 1}$$

where I_{sum} represents the summated CD spectrum with abundance ratio, I_M and I_P represent the CD spectra of *M*-configurated species and *P*-configurated species, respectively, and c_M and c_P represent the abundance ratio of *M*/*P* species satisfying the following equation.

$$c_M + c_P = 1 \quad \cdot\cdot\cdot \text{Equation 2}$$

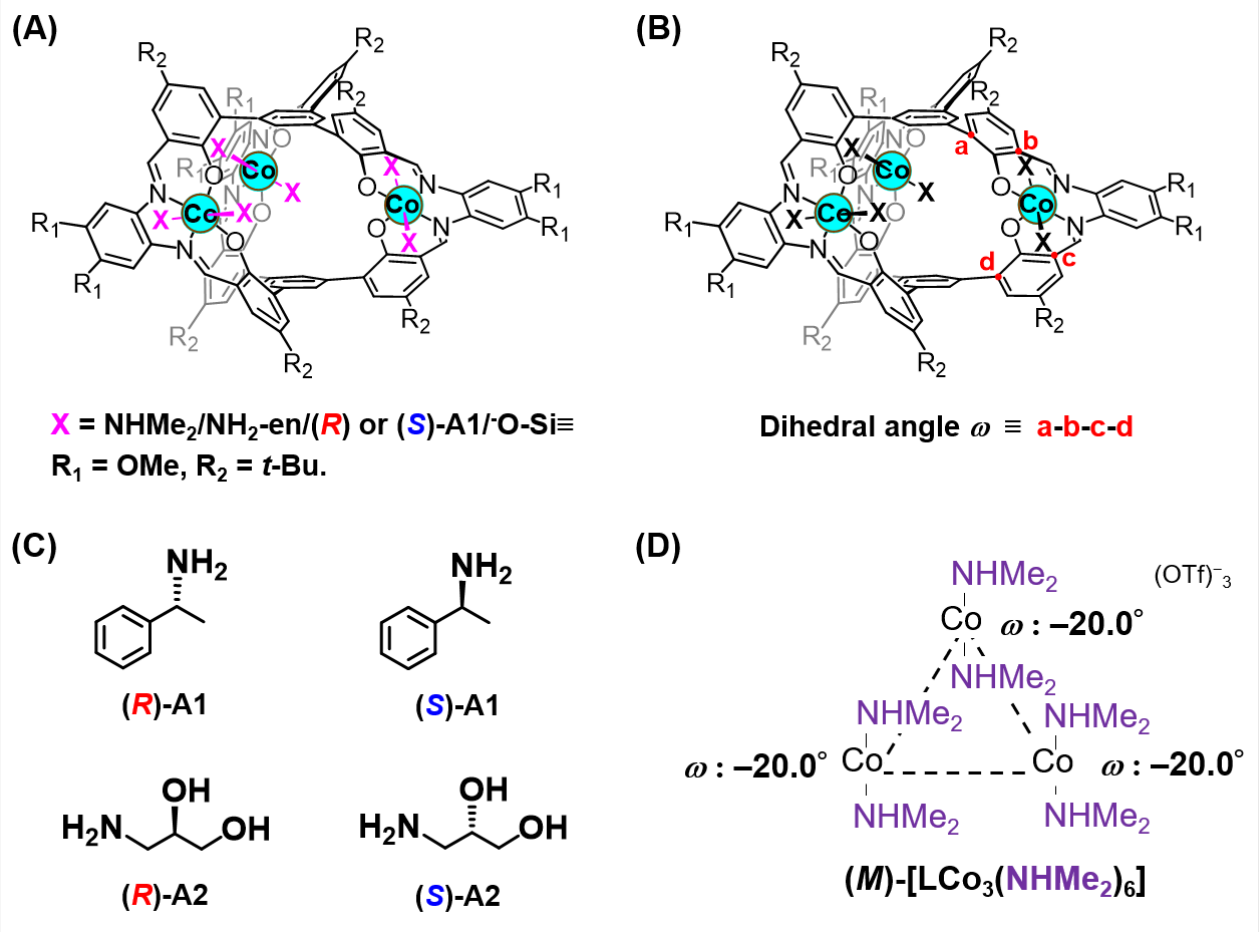

Fig. S2. (A) A chemical structure of (*M*)-$[LCo_3(X)_6]^{3+}$. (B) The torsion angle ω of saloph moiety of the ligand L in (*M*)-$[LCo_3(X)_6]^{3+}$. (C) Chemical structures of the axial ligands. (D) An abbreviated schematic structure of the optimized structure of (*M*)-$[LCo_3(NHMe_2)_6]^{3+}$. ω represents the torsion angle of the saloph moiety as defined in **Fig. S2(B)**.

3. Results and discussion for computational experiments

3.1 Optimized structure, UV-vis and CD spectra of *M* and *P* enantiomers of the trinuclear cobalt complex $[LCo_3(NHMe)_6]^{3+}$ in solution

M- and *P*-configurations of $[LCo_3(NHMe_2)_6]^{3+}$ were fully optimized from the crystal structures of $[LCo_3(NHMe_2)_6](OTf)_3$[3] by simplifying the ligand including solvent effects (acetonitrile) (**Fig. S3(A)**).

Figs. S3(B) and S3(C) show the calculated UV-vis and CD spectra of the *M* and *P* enantiomers of structurally optimized trinuclear cobalt complexes $[LCo_3(NHMe_2)_6]$ in solution (acetonitrile). The UV-vis spectra of these enantiomers were completely identical to each other. The CD spectra, on the other hand, were in a mirror-image as shown in **Fig. S3(C)**. Practically, the CD spectra of $[LCo_3(NHMe_2)_6]^{3+}$ cancelled out in its equilibrium and the Cotton effect was not observed because the *M* and *P* enantiomers equally exist in solution.

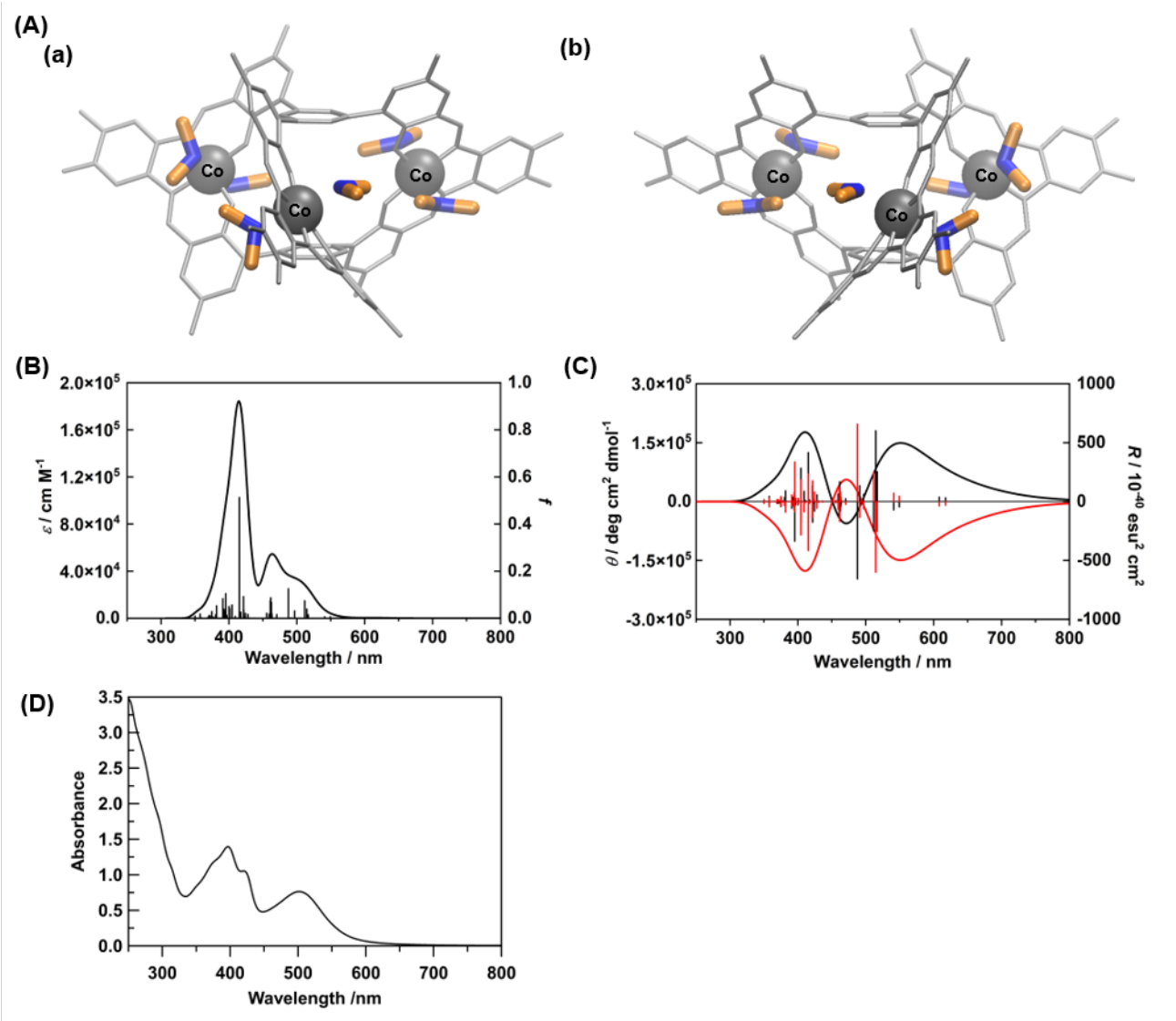

Fig. S3. (A) Optimized structures of (a) *M*- and (b) *P*-configurations of $[LCo_3(NHMe_2)_6]^{3+}$. Gray ball: Co atom, gray stick: ligand L, blue: N atom of $NHMe_2$, orange: methyl group of $NHMe_2$. H atoms are omitted for clarity. Calculated (B) UV-vis and (C) CD spectra of the enantiomers of $[LCo_3(NHMe_2)_6]^{3+}$. Black and red lines are the CD spectra of the *M* and *P* enantiomers, respectively. (D) An experimental UV-vis spectrum of $[LCo_3(NHMe_2)_6](OTf)_3$ in methanol (c = 0.2 mol L^{-1}).

3.2 Optimized structure, UV-vis and CD spectra of the trinuclear cobalt complex $[LCo_3((R)\text{-}\mathbf{A1})_6]^{3+}$

The structure of trinuclear cobalt complex $[LCo_3((R)\text{-}\mathbf{A1})_6]^{3+}$ was fully optimized by replacing $NHMe_2$ of $(M/P)\text{-}[LCo_3(NHMe_2)_6]^{3+}$ to (*R*)-**A1**. The single crystal structure of $[LCo_3((R)\text{-}\mathbf{A1})_6]$ $(OTf)_3$ has been reported, and the configuration was determined to be (*M*) isomer.[3]

The substitution of Me_2NH in $(M)\text{-}[LCo_3(NHMe_2)_6]^{3+}$ by (*R*)-**A1** stabilized the complex by 0.83 kcal/mol in Gibbs free energy, indicating that achiral $NHMe_2$ was easily substituted by chiral **A1** in solution.

Two helical isomers, $(M)\text{-}[LCo_3((R)\text{-}\mathbf{A1})_6]^{3+}$ and $(P)\text{-}[LCo_3((R)\text{-}\mathbf{A1})_6]^{3+}$ in vacuum were simulated to examine the effects of helicity of the complex (*M* or *P*) on the spectra (**Fig. S4(A)**). In the local minimum structure, the (*M*) isomer was more stable by 6.21 kcal/mol than the (*P*) isomer. These results supported the formation of single crystal structure of the (*M*) isomer.[3]

The calculated UV-vis and CD spectra of trinuclear cobalt complex $(M)\text{-}[LCo_3((R)\text{-}\mathbf{A1})_6]^{3+}$ in solution (**Fig. S4(B,C)**) were compared with the experimental spectra in **Fig. S4(D,E)**. The theoretical calculations suitably reproduced the observed UV-vis and CD spectra in solution with respect to the peak position, intensity and the Cotton effects.

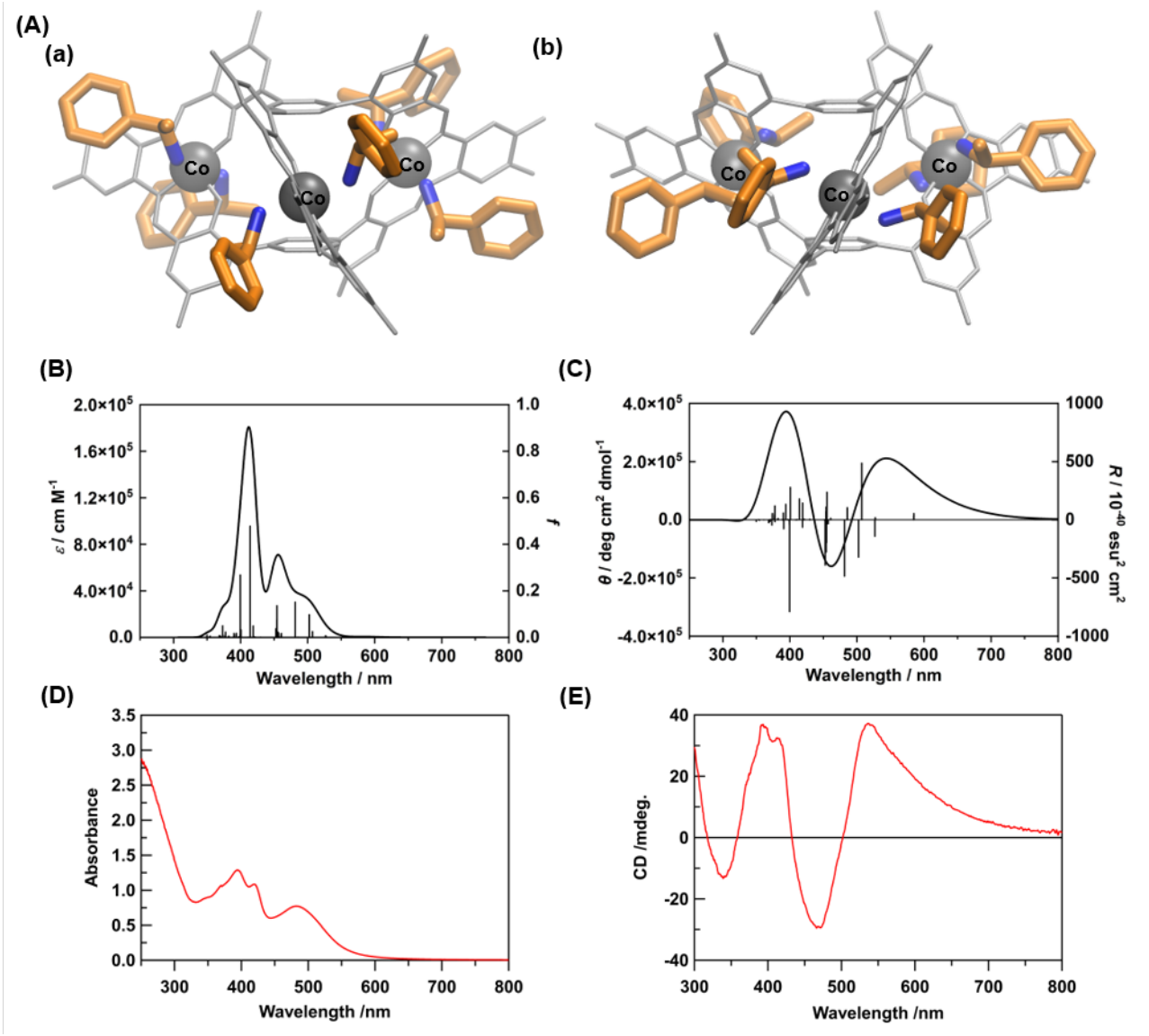

Fig. S4. (A) Optimized structures of (a) (*M*)-$[LCo_3((R)\text{-}\mathbf{A1})_6]^{3+}$ and (b) (*P*)-$[LCo_3((R)\text{-}\mathbf{A1})_6]^{3+}$. Gray ball: Co atom, gray stick: ligand L, blue: N atom of (*R*)-**A1**, orange: methyl and phenyl groups of (*R*)-**A1**. H atoms are omitted for clarity. (B) A calculated UV-vis spectrum of (*M*)-$[LCo_3((R)\text{-}\mathbf{A1})_6]^{3+}$. (C) A calculated CD spectrum of (*M*)-$[LCo_3((R)\text{-}\mathbf{A1})_6]^{3+}$. (D) An experimental UV-vis spectrum of (*M*)-$[LCo_3((R)\text{-}\mathbf{A1})_6]^{3+}$ in methanol (c = 0.2 mol L^{-1}). (E) An experimental CD spectrum of (*M*)-$[LCo_3((R)\text{-}\mathbf{A1})_6]^{3+}$ in methanol (c = 0.2 mol L^{-1}).[3]

3.3 Effects of the linker (en) binding to silica surface on UV-vis and CD spectra

Coordination of the linker (en) to one of Co sites in $[LCo_3((R)\text{-}\mathbf{A1})_6]^{3+}$ was investigated by the exchange of one of the coordinated **A1** to en. The effects of the coordination of en to the absorption and CD spectra were investigated by comparing these spectra of trinuclear cobalt complexes $(M)\text{-}[LCo_3((R)\text{-}\mathbf{A1})_6]^{3+}$ and $(M)\text{-}[LCo_3en((R)\text{-}\mathbf{A1})_5]^{3+}$ (**Fig. 2(B)(a,b)** in the main text).

The calculated stabilization energy was 1.95 kcal/mol in the ligand exchange in which one of the **A1** ligands in $(M)\text{-}[LCo_3((R)\text{-}\mathbf{A1})_6]^{3+}$ was replaced by en. Therefore, it was expected that the axial ligand of $(M)\text{-}[LCo_3((R)\text{-}\mathbf{A1})_6]^{3+}$ was exchanged from **A1** to en and the trinuclear complex would be immobilized to the surface with the en linker. The calculated UV-vis and CD spectra of $(M)\text{-}[LCo_3((R)\text{-}\mathbf{A1})_6]^{3+}$ and $(M)\text{-}[LCo_3en((R)\text{-}\mathbf{A1})_5]^{3+}$ were almost the same, which means that the influence of coordination of the linker on the spectra was negligible.

3.4 A surface structural model of $LCo_3((R)$-A1)/en-SiO_2 with the coordination of –O-$Si(OH)_3$ group representing silica surface, and calculated UV-vis and CD spectra

The effect of the coordination of silanol (Si-OH) to one of the Co sites in $[LCo_3]$ unit was next investigated by the exchange of one of the coordinated ligands to Si-OH. As mentioned in sections **3.2** and **3.3**, the positions of the two ligands ($NHMe_2$ and ((*R*)-**A1**) did not affect much on the calculated UV-vis and CD spectra. Therefore, a simplified model of surface-attached structure of $[LCo_3]$ unit was designed, which was denoted as "**$LCo_3((R)$-A1)/en-SiO_2_calc**" as shown in **Fig. 2**. We optimized both *M* and *P* configurations of **$LCo_3((R)$-A1)/en-SiO_2_calc**.

The calculated UV-vis spectra of **$LCo_3((R)$-A1)/en-SiO_2_calc** (*M*- and *P*-configurations) were shown in **Fig. 2(C)(a)** in the main text, indicating that the difference was minor. The calculated CD spectra of **$LCo_3((R)$-A1)/en-SiO_2_calc** (*M*- and *P*-configurations) were shown in **Fig. 2(C)(b)** in the main text, which showed weak positive Cotton effect at around 400 nm, and the Cotton effect at around 630 nm became major.

3.5 Simulation of CD spectra with abundance ratio of the (*M*) and (*P*)-configurated species

We simulated the CD spectra of **LCo3((*R*)-A1)/en-SiO2_calc** by considering the abundance ratios of the *M* and *P*-configurated species. The simulation of CD spectra was conducted using equation 1. **Fig. S5** shows the simulated CD spectra with different *M*/*P* ratios. The simulated CD spectrum showed a characteristic peak at 500-600 nm and almost negligible peak at 350-450 nm when *M*/*P* ratio was 55/45 (**Fig. 2(D)** in the main text).

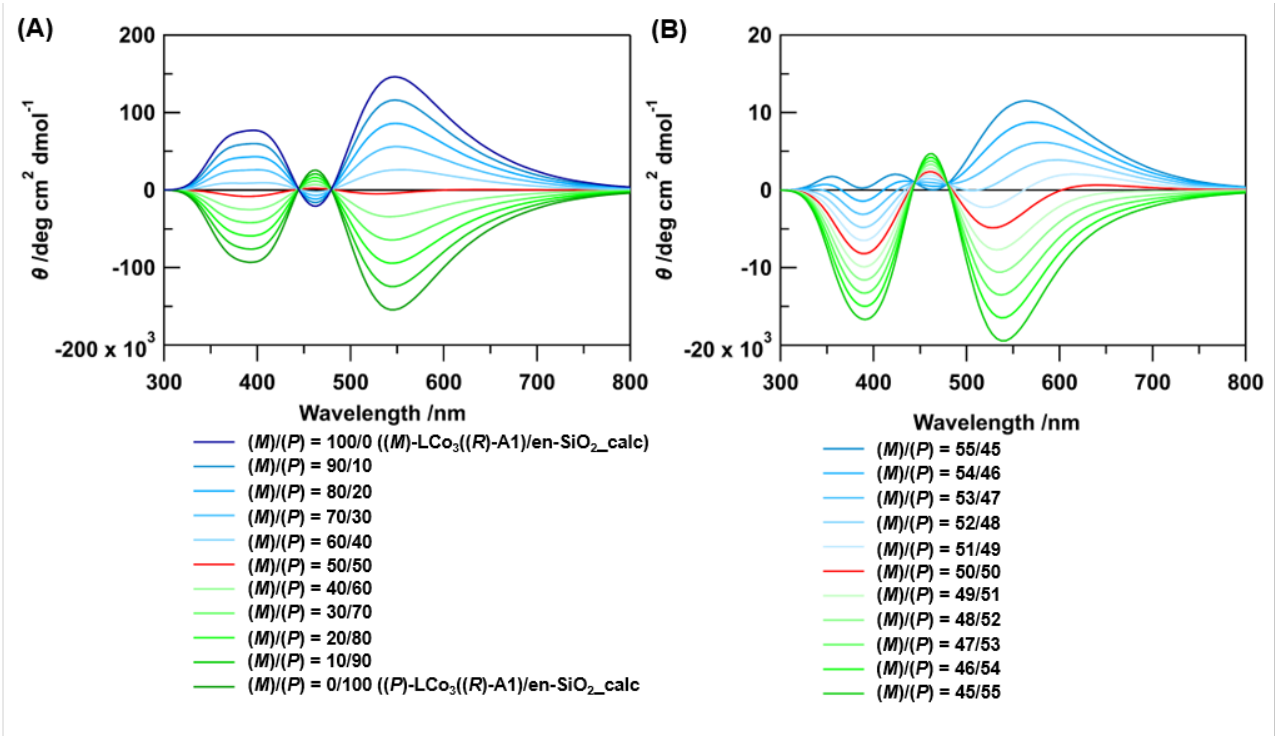

Fig. S5. The simulated CD spectra of **LCo3((*R*)-A1)/en-SiO2_calc** (*M*- and *P*-configurations) and **LCo3((*R*)-A1)/en-SiO2_calc** with different *M*/*P* ratios. (A) *M*/*P* = 90/10 ~ 10/90, (B) *M*/*P* = 55/45 ~ 45/55.

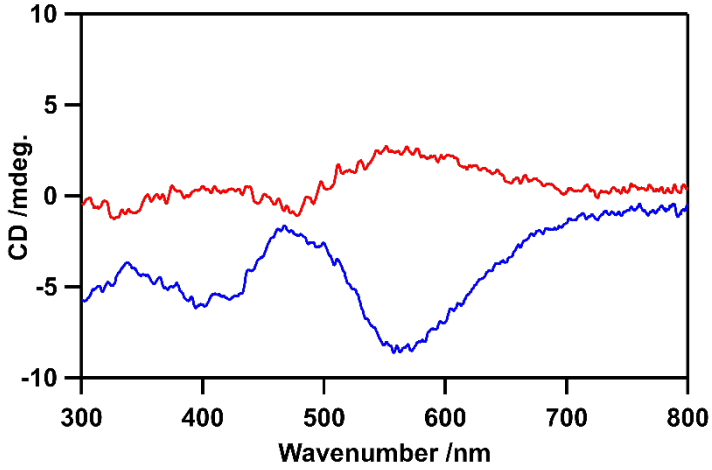

Fig. S6. DR CD spectra of **LCo_3((*R*)-A1)/en-SiO_2** (blue) after the addition of an excess amount (100 eq. to [LCo_3] unit) of (*S*)-**A2**, and **LCo_3((*S*)-A1)/en-SiO_2** (red) after the addition of excess amount (100 eq. to [LCo_3] unit) of (*R*)-**A2**.

References

1. S. Akine, M. Miyashita, T. Nabeshima, *J. Am. Chem. Soc.* 2017, **139**, 4631.
2. S. Akine, M. Miyashita, T. Nabeshima, *Chem. Eur. J.* 2019, **25**, 1432.
3. Y. Sakata, S. Chiba, M. Miyashita, T. Nabeshima, S. Akine, *Chem. Eur. J.* 2019, **25**, 2962.
4. S. Akine, M. Miyashita, T. Nabeshima, *Inorg. Chem.* 2021, **60**, 12961.
5. (a) B. Ravel, M. Newville, *J. Synchrotron Rad.* 2005, **12**, 537–541. (b) M. Newville, B. Ravel, D. Haskel, J. J. Rehr, E. A. Stern, Y. Yacoby, *Physica B* 1995, **208–209**, 154–156.
6. J. A. Bearden, A. F. Burr, *Rev. Mod. Phys.* 1967, **39**, 125–142.
7. (a) M. Newville, *J. Synchrotron Rad.* 2001, **8**, 322–324. (b) M. Newville, P. Līviņš, Y. Yacoby, J. J. Rehr, E. A. Stern, *Phys. Rev. B: Condens. Matter Mater. Phys.* 1993, **47**, 14126–14131.
8. (a) A. D. Becke, J. *Chem. Phys.* 1993, **98**, 1372. (b) C. Lee, W. Yang, R. G. Parr, *Phys. Rev.* B 1998, **37**, 785.
9. (a) J. Tomasi, B. Mennucci, R. Cammi, *Chem. Rev.* 2005, **105**, 2999. (b) B. Mennucci, E. Cancès, J. Tomasi, *J. Phys. Chem. B* 1997, **101**, 10506.
10. (a) P. Fuentealba, H. Preuss, H. Stoll, L. V. Szentpály, *Chem. Phys. Lett.*, 1982, **89**, 418. (b) M. Dolg, U. Wedig, H. Stoll, H. Preuss, *J. Chem. Phys.* 1987, **86**, 866.
11. P. J. Stephens, N. Harada, *Chirality.* 2010, **22**, 229.
12. M. J. Frisch, G. W. Trucks, H. B. Schlegel, G. E. Scuseria, M. A. Robb, J. R. Cheeseman, G. Scalmani, V. Barone, G. A. Petersson, H. Nakatsuji, X. Li, M. Caricato, A. V. Marenich, J. Bloino, B. G. Janesko, R. Gomperts, B. Mennucci, H. P. Hratchian, J. V. Ortiz, A. F. Izmaylov, J. L. Sonnenberg, D. Williams-Young, F. Ding, F. Lipparini, F. Egidi, J. Goings, B. Peng, A. Petrone, T. Henderson, D. Ranasinghe, V. G. Zakrzewski, J. Gao, N. Rega, G. Zheng, W. Liang, M. Hada, M. Ehara, K. Toyota, R. Fukuda, J. Hasegawa, M. Ishida, T. Nakajima, Y. Honda, O. Kitao, H. Nakai, T. Vreven, K. Throssell, J. A. Montgomery, Jr., J. E. Peralta, F. Ogliaro, M. J. Bearpark, J. J. Heyd, E. N. Brothers, K. N. Kudin, V. N. Staroverov, T. A. Keith, R. Kobayashi, J. Normand, K. Raghavachari, A. P. Rendell, J. C. Burant, S. S. Iyengar, J. Tomasi, M. Cossi, J. M. Millam, M. Klene, C. Adamo, R. Cammi, J. W. Ochterski, R. L. Martin, K. Morokuma, O. Farkas, J. B. Foresman, and D. J. Fox, *Gaussian 16*, Revision A.03, Gaussian, Inc., Wallingford CT, 2016.
13. W. Humphrey, A. Dalke, K. Schulten, *J. Molec. Graphics*, 1996, **14**, 33-38.